


RESEARCH ARTICLE

Positron emission tomography visualized stimulation of the vestibular organ is localized in Heschl's gyrus

Louise Devantier^{1,2}  | Allan K. Hansen³ | Jens-Jacob Mølby-Henriksen² | Christian B. Christensen⁴ | Michael Pedersen⁵ | Kim V. Hansen³ | Måns Magnusson⁶ | Therese Ovesen^{1,2} | Per Borghammer³

¹Department of Clinical Medicine, Aarhus University, Aarhus, Denmark

²Department of Oto-Rhino-Laryngology, Regional Hospital West Jutland, Holstebro, Denmark

³Department of Nuclear Medicine & PET Centre, Aarhus University Hospital, Aarhus, Denmark

⁴Department of Engineering, Aarhus University, Aarhus, Denmark

⁵Comparative Medicine Lab, Aarhus University, Aarhus, Denmark

⁶Department of Oto-Rhino-Laryngology, Lund University Hospital, Lund, Sweden

Correspondence

Louise Devantier, Department of Clinical Medicine, Aarhus University, Palle Juul-Jensens Blvd. 82, 8200 Aarhus N, Denmark.
Email: louise.devantier@aarhus.rm.dk

Funding information

Aase and Ejnar Danielsen's Foundation; Hans Skouby's Foundation; Health Research Fund of Central Denmark Region; Knud and Edith Eriksen's Memorial Foundation; The A.P. Møller Foundation for the Advancement of Medical Science; The Augustinus Foundation; The Ménière and tinnitus Foundation; The Oticon Foundation; The Toyota Foundation

Abstract

The existence of a human primary vestibular cortex is still debated. Current knowledge mainly derives from functional magnetic resonance imaging (fMRI) and positron emission tomography (PET) acquisitions during artificial vestibular stimulation. This may be problematic as artificial vestibular stimulation entails coactivation of other sensory receptors. The use of fMRI is challenging as the strong magnetic field and loud noise during MRI may both stimulate the vestibular organ. This study aimed to characterize the cortical activity during natural stimulation of the human vestibular organ. Two fluorodeoxyglucose (FDG)-PET scans were obtained after natural vestibular stimulation in a self-propelled chair. Two types of stimuli were applied: (a) rotation (horizontal semicircular canal) and (b) linear sideways movement (utricle). A comparable baseline FDG-PET scan was obtained after sitting motion-less in the chair. In both stimulation paradigms, significantly increased FDG uptake was measured bilaterally in the medial part of Heschl's gyrus, with some overlap into the posterior insula. This is the first neuroimaging study to visualize cortical processing of natural vestibular stimuli. FDG uptake was demonstrated in the medial-most part of Heschl's gyrus, normally associated with the primary auditory cortex. This anatomical localization seems plausible, considering that the labyrinth contains both the vestibular organ and the cochlea.

KEYWORDS

central nervous system, functional neuroimaging, labyrinth, neurotology, positron-emission-tomography, vertigo, vestibule

1 | INTRODUCTION

All sensory systems except the vestibular system have been localized to specific cortical areas of the human brain. The existence of a distinct vestibular cortex, however, is still being debated (zu Eulenburg, Caspers, Roski, & Eickhoff, 2012). Animal studies have shown that several areas in

the temporal and parietal cortex receive afferents from the vestibular nuclei. The superior temporal gyrus, inferior parietal lobule (angular and supramarginal gyrus), somatosensory cortex, precuneus, cingulate gyrus, frontal cortex (motor cortex and frontal eye fields), hippocampus, thalamus, and in particular, cortex at the parietoinsular intersection have all been suggested to take part in the human vestibular cortical network

This is an open access article under the terms of the Creative Commons Attribution-NonCommercial-NoDerivs License, which permits use and distribution in any medium, provided the original work is properly cited, the use is non-commercial and no modifications or adaptations are made.

© 2019 The Authors. *Human Brain Mapping* published by Wiley Periodicals, Inc.

(Lopez & Blanke, 2011). The latter has been defined as the parietoinsular vestibular cortex (PIVC) by several researchers and is believed to constitute a critical node for processing vestibular stimuli (Guldin & Grusser, 1998). Electrophysiological experiments in monkeys have shown that cortical neurons in the PIVC responding to vestibular stimulation also responded to optokinetic and somatosensory stimuli (Grusser, Pause, & Schreiter, 1990b). However, studies on macaques demonstrated that the vast majority of neurons in the PIVC only responded to well-defined vestibular stimuli (Chen, DeAngelis, & Angelaki, 2010).

Current knowledge of vestibular cortical processing in humans is primarily based on positron emission tomography (PET) or functional magnetic resonance imaging (fMRI). Although a recent meta-analysis of 28 imaging studies supported the existence of a unique and distinct vestibular cortex in humans located in the parietal operculum (zu Eulenburg et al., 2012), all these studies utilized artificial stimulation of the vestibular organ without physical head motion, by caloric irrigation, galvanic stimulation, or loud sound, as used in the test of vestibular-evoked myogenic potentials (VEMP).

The validity of such artificial vestibular stimulations and the use of fMRI in the context of studying vestibular function could be challenged or at least considered incomplete. The caloric stimulus may lead to potentially confounding coactivation of vagal, thermal, nociceptive, and sensory systems (zu Eulenburg, Muller-Forell, & Dieterich, 2013), and the strong static magnetic field of MRI systems could mediate independent vestibular stimuli, as it can trigger nystagmus (Mian, Li, Antunes, Glover, & Day, 2013; Roberts et al., 2011). fMRI examinations also require the subject to lie motionless inside the magnet during image acquisition, precluding natural stimulation of the vestibular system, such as head movements. In contrast, PET scans are better suited for this type of study. PET allows imaging of the radioactive glucose analog ^{18}F -fluorodeoxyglucose (FDG) and is an established method for brain activation studies (Villien et al., 2014). ^{18}F -FDG is injected and irreversibly trapped in neurons in proportion to the neuroenergetic requirements of activated brain structures. This method allows activation paradigms to be performed outside the scanner. Subsequently, the PET scan reveals the relative glucose uptake in brain regions produced by that specific paradigm. As an example, ^{18}F -FDG PET has been used to map cortical activation patterns while subjects were running or driving a car (Jeong et al., 2006; Tashiro et al., 2001).

The objectives of this study were: (a) to validate a natural stimulus paradigm of the human vestibular organ outside the PET scanner and (b) to subsequently obtain ^{18}F -FDG PET scans to map regional activation patterns in the brain during that stimulation. Using a natural vestibular stimulation, resembling a "real-world" stimulation paradigm, we hypothesized that such stimulus leads to increased metabolism in the posterior insula and neighboring area.

2 | MATERIALS AND METHODS

2.1 | Subjects

A total of 14 healthy volunteers were recruited (8 females; age: 50–60 years, mean age 55.1 ± 3.0 years). All participants were

interviewed via telephone to exclude previous medical history with dizziness, neurological or psychiatric disorders of any kind, and use of potential neuromodulating medication. Only right-handed volunteers according to the 10-item inventory of the Edinburg test (Oldfield, 1971) and nonsmokers were included in the study. Cervical VEMP, ocular VEMP (Curthoys, 2017) (Eclipse, Interacoustics, Middelfart, Denmark), and video head impulse test (EyeSeeCam, Interacoustics, Middelfart, Denmark) were carried out prior to the PET examinations to ensure normal function of the vestibular organ (Halmagyi et al., 2017). All 14 healthy volunteers were included in the study and underwent three ^{18}F -FDG-PET scans. Informed oral and written consent were obtained from all participants. The study was approved by the Central Region of Denmark Research Ethics Committee (no: 1-10-72-135-16). The results of the study are reported in agreement with the STROBE statement (von Elm et al., 2014).

2.2 | ^{18}F -FDG-PET procedures

The participants were seated and strapped in as comfortable as possible in a custom-designed self-propelled chair (Figure 1). The head was tilted downward approximately 20° and fixated with a headgear. To avoid visual stimulation and minimize auditory input, all participants wore sleep-goggles and noise-canceling in-ear headphones (QuietControl 30 wireless headphones, Bose, Framingham, U.S.) during all three stimulation paradigms. Participants underwent three ^{18}F -FDG PET scans at three separate days, due to the extended radioactive half-life of ^{18}F (110 min) preventing multiple same-day PET examinations. Each subject had one baseline PET scan and PET scans after linear and rotational stimulation of the vestibular organ, respectively. The order of the three stimulation paradigms was randomized. The participants fasted for 6 hr prior to a bolus injection of radioactive ^{18}F -FDG (170 MBq [$\pm 10\%$]) into a cubital vein. After the baseline or stimulation condition was concluded, the participants were transferred to the PET facility.

2.3 | Vestibular stimulation

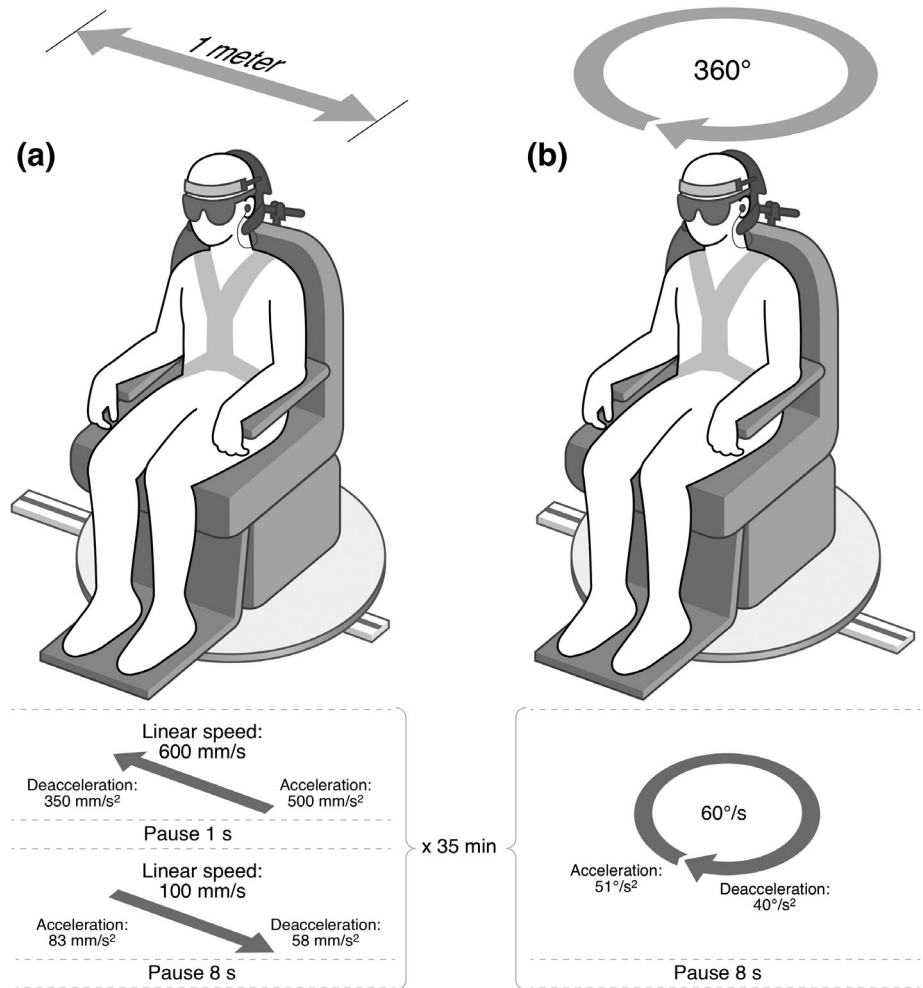
2.3.1 | Linear stimulation

Immediately after ^{18}F -FDG injection, the chair was set in motion and continuous stimulation applied for 35 min. The chair performed a rapid linear acceleration (acceleration: 500 mm/s^2 , speed: 600 mm/s) toward the right with the patient immobilized in a face-forward position and then paused for 1 s before slowly (acceleration: 83 mm/s^2 , speed: 100 mm/s) returning to the starting position. This movement pattern was repeated for 35 min (Figure 1).

2.3.2 | Rotatory stimulation

Immediately after the ^{18}F -FDG injection, rotational stimulation was applied by 360° clockwise rotations of the chair followed by an 8 s pause before initiating the next rotation (acceleration: $51^\circ/\text{s}^2$, speed: $60^\circ/\text{s}$). The chair repeated this pattern for 35 min (Figure 1). Videos

FIGURE 1 The self-propelled chair. The participants were strapped in the chair and wore noise-canceling earphones and sleep-goggles during vestibular stimulation. Linear stimulation: The chair moved rapidly to the right (acceleration: 500 mm/s^2 , speed: 600 mm/s) then paused for 1 s before slowly (acceleration: 83 mm/s^2 , speed: 100 mm/s) returning to the starting position. This movement pattern was repeated for 35 min. The chair performed cycles of rapid rightward movements and slow leftward movements during 35 min of stimulation in order to create a predominantly right-sided utricular stimulus. Rotatory stimulation: The chair rotated 360° clockwise (acceleration: $51^\circ/\text{s}^2$, speed: $60^\circ/\text{s}$) followed by an 8 s pause before initiating the next rotation. The chair repeated this pattern for 35 min. The chair performed clockwise rotations in order to create a predominantly right-sided stimulus of the semicircular canal



of the linear and circular stimulations are available in the Supporting Information.

2.4 | Baseline condition

Participants were positioned and strapped into the chair and wore sleep-goggles and noise-cancellation headphones. The ^{18}F -FDG was injected and the chair was kept motionless for 35 min.

2.5 | Noise measurements

Due to the close anatomical relationship between the posterior insula and the primary auditory cortex (Heschl), we were aware that noise could confound the results by giving rise to increased FDG uptake in the auditory cortex, despite our attempts to construct a silent chair and the use of noise-cancellation ear plugs. To facilitate interpretation of our imaging data, we therefore performed measurements of ambient noise levels and the noise produced by the chair using an artificial ear and cheek simulator (43AG, G.R.A.S. Sound and Vibration, Holte, Denmark) combined with an ESI U46 XL soundcard (ESI, ESI Audiotechnik GmbH, LeonBerg, Germany). Due to the tonotopic arrangement of the auditory cortex, we paid particular attention to measuring the frequency.

2.6 | PET acquisition

Immediately after each of the three stimulation conditions, participants were transferred to a wheel chair and transported to the PET facility with noise-cancellation earphones and eye covers still in place to minimize motor activity and feedback and sensory inputs. Participants were placed on the bed and a 6-min transmission scan (^{137}Cs point source) was initiated at 54 min postinjection. Exactly 60 min postinjection, a 60-min dynamic PET acquisition (12×5 min frames) was performed on a high-resolution PET system (ECAT HRRT; CTI/Siemens, Knoxville, TN) Full scanner details have been published previously (Heiss et al., 2004). The PET scans were reconstructed using an ordered-subsets expectation maximization three-dimensional (3D) algorithm into image volumes consisting of 207 axial slices and a 1.22 mm voxel size. Reconstructed images were corrected for random and scatter events, detector efficiency variations, and dead time. Frame-to-frame motion correction was performed followed by summation of all frames into one static PET data volume.

2.7 | MRI acquisition

MRI was performed with a clinically available 3 T system (Siemens Skyra, Siemens Healthcare, Erlangen, Germany) and image reception as

performed with a 32-element head-coil. The following sequences were performed. First, a T2-weighted spin-echo sequence was employed in axial direction for high-resolution imaging of the inner ear, using the following parameters: TE = 152 ms, TR = 4,540 ms, image resolution $0.9 \times 0.9 \times 0.9 \text{ mm}^3$, and acquisition time = 5.5 min. Second, a 3D T1-weighted gradient-echo sequence was acquired to cover the entire brain using the parameters: TE = 1.5 ms, TR = 16 ms, flip angle = 15° , $0.9 \times 0.9 \times 0.9 \text{ mm}^3$, and acquisition time = 5 min.

2.8 | Data analysis

Using SPM12 (<https://www.fil.ion.ucl.ac.uk/spm/>) for MATLAB (MathWorks, Natick, MA), the three PET image volumes of each participant were coregistered to common stereotactic space (MNI space) via the individual's MRI. Automated gray matter-white matter segmentation was performed on the T1-weighted MRI images. To minimize effects of irrelevant global scaling factors in the ^{18}F -FDG activity levels, the ^{18}F -FDG values were intensity normalized (using ratio normalization) to the mean activity level of the total gray matter by applying a gray matter volume of interest (VOI), thus obtaining standard uptake value ratio (SUVR) maps. To map the effect of each stimulation in each subject, baseline maps were subtracted from stimulation maps ($\Delta\text{SUVR} = \text{SUVR}_{\text{stimulation}} - \text{SUVR}_{\text{baseline}}$).

Parametric maps were smoothed using a 12-mm Gaussian filter, before voxel-based statistical analysis. To test the a priori hypothesis, we applied predefined VOIs using SPM's built-in atlas, that is, posterior insula and the neighboring Heschl's gyrus and extracted averaged SUVR values from these VOIs. In addition, a whole-brain SPM analysis of the ^{18}F -FDG ΔSUVR images from each type of stimulation was performed within all gray matter voxels using simple voxel-wise statistical t tests. Multiple comparison correction was performed using the built-in family-wise error (FWE) correction with a threshold of $p < .05$.

The labels shown in Figure 2 are from SPM's built-in atlas.

Because the FWE correction of SPM is often overly conservative, we performed additional explorative whole-brain surface-based tests in FreeSurfer (<https://surfer.nmr.mgh.harvard.edu>). T1-weighted MRI was imported using the standard pipeline, ΔSUVR maps were created and coregistered to MRI in SPM12. Using FreeSurfer, the ΔSUVR values within the cerebral cortex, as defined by MRI, were projected onto a surface, which is then transformed into a common surface. Data points on the surfaces were then interrogated using a general linear model. Clusters were defined using one-sided p values from a vertex-wise z -map thresholded at $p = .05$, and subsequently corrected for multiple comparisons using FreeSurfer's precomputed Z Monte Carlo simulation, based on Hagler, Saygin, and Sereno

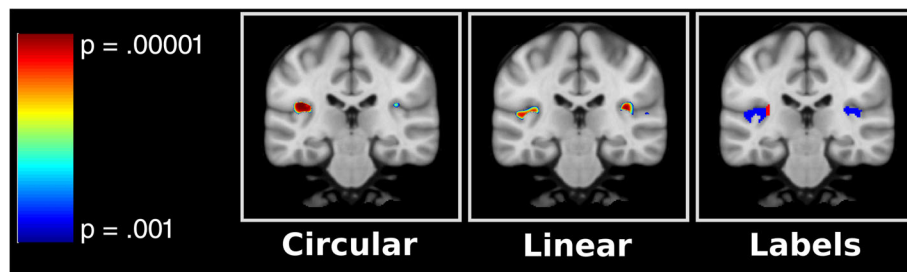


FIGURE 2 Uncorrected p maps from the SPM analyses. In both the circular and linear stimulation, increased ^{18}F -FDG was evident in the intersection between Heschl's gyrus and the posterior insula. Labels on the right side shows the anatomical regions as defined in the SPM atlas (blue label = Heschl's gyrus; red label = posterior insula)

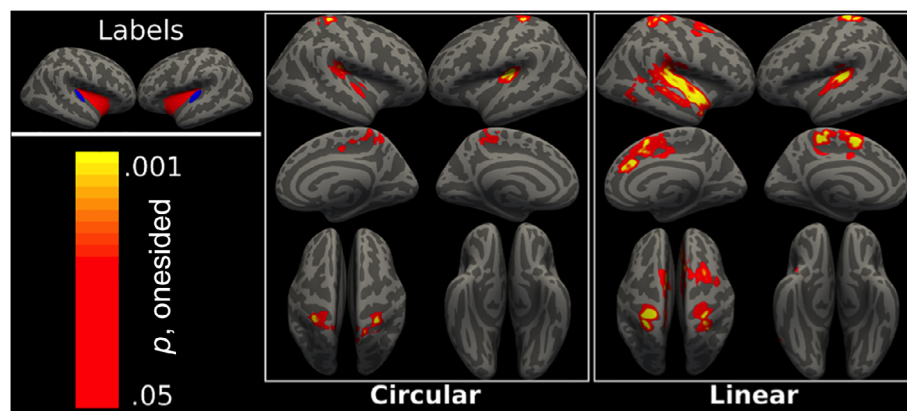


FIGURE 3 Surface-based analysis. Whole-brain surface-based analysis in FreeSurfer showing clusters with increased ^{18}F -FDG uptake in circular or linear stimulation. Only clusters surviving cluster-wise multiple comparison correction are shown. Uncorrected p values are superimposed in order to show that data structure inside these clusters. For example, it seems that the deep part of Heschl's gyrus displays a high-magnitude change bilaterally in the linear stimulus condition and in the left side during the circular stimulus condition. Upper left shows labels for anatomical orientation. Blue is Heschl's gyrus and red is insula, as defined by the Desikan-Killeany atlas. Dark gray is sulci and light gray is gyri. Color scale on lower left applies to both circular and linear surface maps

TABLE 1 Peak MNI coordinates (x y z) from SPM analysis

	MNI coordinates	Anatomical brain areas (BA)
<i>Rotatory stimulation</i>		
Right	37 -29 18	Right auditory cortex (BA 41)
Left	-38 -22 13	Left auditory cortex (BA 41)
<i>Linear stimulation</i>		
Right	38 -30 15	Right auditory cortex (BA 41)
Left	-34 -33 17	Left auditory cortex (BA 41)

Note: The peak ^{18}F -FDG uptake was located in Heschl's gyrus (auditory cortex, BA 41) in both stimulation paradigms.

Abbreviation: BA, Brodmann area.

TABLE 2 Comparison of the linear and rotatory stimulation

	MNI-space coordinates	Anatomical brain areas	Cluster-wise p value
<i>Right hemisphere</i>			
Cluster no. 1	59 -26 7	Right auditory cortex (BA 41)	.00020
<i>Left hemisphere</i>			
Cluster no. 1	-22 20 45	Left BA 8	.00020
Cluster no. 2	-8 0 57	Left BA 6	.00040
Cluster no. 3	-31 3 -41	Left BA 38	.01851

Note: FreeSurfer analysis. MNI coordinates (x y z) are presented from clusters with significantly higher ^{18}F -FDG uptake during the linear stimulation compared with the rotatory stimulation. There were no clusters with significantly higher ^{18}F -FDG uptake during the rotatory stimulation compared with the linear stimulation. Cluster-wise p values are corrected for multiple comparisons.

Abbreviation: BA, Brodmann area.

(2006). Only clusters with cluster-wise-corrected p values $<.05$ are shown. Labels on Figure 3 are from FreeSurfer's built-in atlas (Desikan-Killiany; Desikan et al., 2006). Requests to share study data and analyses results should be addressed to the corresponding author.

3 | RESULTS

3.1 | VOI- and voxel-based analyses

A marked increase in normalized cerebral ^{18}F -FDG uptake was found in the a priori defined VOIs for both the linear stimulation (mean ΔSUVR : Heschl's gyrus 95% confidence interval [CI]: [0.026, 0.056], $p = .0001$; posterior insula 95% CI: [0.002, 0.019], $p = .02$) and rotatory vestibular stimulation (mean ΔSUVR : Heschl's gyrus 95% CI: [0.009, 0.041], $p = .008$; posterior insula 95% CI: [0.007, 0.022], $p = .002$).

Figure 2 shows the anatomical localization of clusters detected using voxel-wise whole-brain SPM analyses. In both stimulus conditions, the uptake was detected bilaterally and predominantly in the deep part of Heschl's gyrus overlapping to some extent with the posterior insula. Peak coordinates were located in Heschl's gyrus (Table 1).

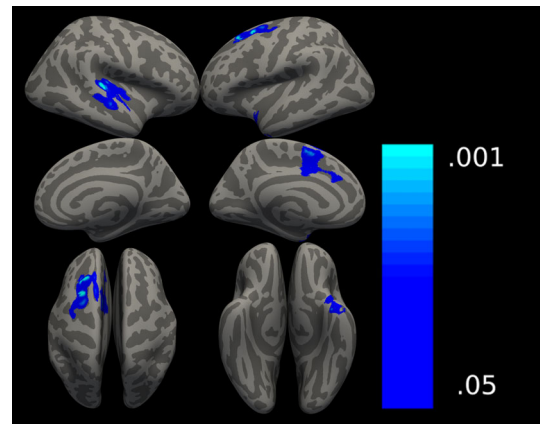


FIGURE 4 Comparison of ^{18}F -FDG uptake between the linear and rotatory stimulation. FreeSurfer analysis showing clusters with significantly higher ^{18}F -FDG uptake during the linear stimulation compared with the rotatory stimulation. There were no clusters with significantly higher ^{18}F -FDG uptake during the rotatory stimulation compared with the linear stimulation

These SPM-derived clusters did, however, not survive correction for multiple comparisons at the voxel level, when family-wise error correction was performed taking all gray matter voxels into account ($p_{\text{FWE-corr}} > .05$).

3.2 | Surface cluster analysis

The whole-brain surface cluster analysis revealed significant increases in the posterior part of insula and the adjoining part of Heschl's gyrus. Additionally, during both rotatory and linear stimulation, significant clusters of activation were detected in the primary motor-sensory cortex with an approximate localization corresponding to the trunk, back, shoulder areas and in premotor cortex and supplementary motor areas (Figure 3). The increased ^{18}F -FDG uptake was more pronounced during the linear stimulation.

3.3 | Comparison of activation during linear versus rotatory stimulation

A comparison of the activation during linear versus rotatory stimulation revealed significant clusters of increased ^{18}F -FDG uptake during linear stimulation compared with rotatory stimulation (Table 2 and Figure 4). Clusters with increased activity were seen in both the right Heschl's gyrus and the left premotor cortex and supplementary motor areas. Only clusters surviving correction for multiple comparisons are displayed.

3.4 | Noise measurements

The chair produced no measurable high-frequency sound and only a relatively small amplitude of low-frequency sound (Supporting Information Figure S2).

4 | DISCUSSION

This ^{18}F -FDG PET study demonstrated regional activation patterns in the human brain during natural vestibular stimulation, suggesting that the most medial part of Heschl's gyrus and the posterior insula are core structures for processing information from the vestibular organs. We found that both linear and rotation accelerations gave rise to activations in these regions. To our knowledge, previous neuroimaging studies in humans have all employed artificial stimulation paradigms without any physical head motion for studying vestibular function. The vast majority of imaging studies on vestibular central processing have used fMRI or ^{15}O -labeled H_2O PET scans. The ^{15}O -labeled H_2O tracer has a short half-life (about 2 min) compared with the ^{18}F -FDG tracer, and thus, it does not allow for natural vestibular stimulation outside the PET system. The spatial resolution in these ^{15}O -labeled H_2O PET images is inferior to high-resolution ^{18}F -FDG PET and fMRI (Kameyama, Murakami, & Jinzaki, 2016; Varrone et al., 2009). fMRI, conversely, has a good temporal resolution, and its spatial resolution is compatible with high-resolution ^{18}F -FDG PET (Kameyama et al., 2016; Varrone et al., 2009). As a neuroimaging technique, fMRI has the advantage over PET that it does not expose research participants to radiation. However, the fMRI design does not permit the use of natural vestibular stimulation. The use of artificial vestibular stimulation poses a problem due to the potentially confounding coactivation of vagal, thermal, nociceptive, and sensory systems (zu Eulenburg et al., 2013), and we believe that fMRI as a neuroimaging technique may also prove to be problematic. It has recently become evident that the strong magnetic field (1.5 T and above) in MRI systems stimulates the vestibular organ by means of Lorentz forces. In the MRI system, a robust nystagmus is elicited in vestibularly healthy humans, and the accompanied nystagmus seems to be dependent on the direction and strength of the magnetic field (Ward, Roberts, Della Santina, Carey, & Zee, 2015). Thus, we argue that conventional fMRI studies concomitant with vestibular activation might be biased by the inherent static magnetic field in the MRI systems, although this hypothesis requires further research (Boegle, Stephan, Ertl, Glasauer, & Dieterich, 2016). Another potential confounding problem with fMRI studies in this research area is the auditory stimulus produced by the gradients coils during fMRI acquisition. Peak gradient-noise level during fMRI in a 3 T MRI has been measured up to 138 dB SPL (Ravicz & Melcher, 2001). Even with earmuffs and earplugs used together, there is still a substantial problem with bone-conducted sound/vibration through the head and body during fMRI acquisition (Ravicz & Melcher, 2001). The bone-conducted vibration during fMRI acquisition is in particular a potential confounding problem in vestibular research as even a small bone-conducted stimulus has been shown to produce a large increase in the firing rate of otolithic receptors (Curthoys & Vulovic, 2011).

Interestingly, the VOI analysis revealed that vestibular stimulations increased ^{18}F -FDG uptake more in Heschl's gyrus than posterior insula. This finding was corroborated by the SPM analysis showing elevated ^{18}F -FDG uptake predominantly in the medial-most part of Heschl's gyrus (Supporting Information Figure S1). This finding

contradicts some previous studies including a meta-analysis, which identified the posterior insula and retroinsular area as potential core vestibular cortical regions (Dieterich & Brandt, 2018; zu Eulenburg et al., 2012). Electrophysiological responses measured during natural vestibular stimulation on motion platforms in non-human primates supported that the posterior insula is a core area for processing vestibular stimuli (Shinder & Newlands, 2014). In the Java monkey, the PIVC was described to be located between a pure somatosensory and pure auditory region during somatosensory, optokinetic, and vestibular stimulation. The auditory region was assigned to be a pure auditory area as they found a response to noise like clapping, whistling, or tone burst in this region (Grusser, Pause, & Schreiter, 1990a). The auditory stimuli are not described in further detail than the above. Whistling, clapping, and tone burst could in addition to being auditory stimuli also be otolith stimuli (Curthoys, 2017) and thus this area could represent both auditory and vestibular processing. The PIVC as a multi-vestibular area was later located in the temporal bank of the lateral sulcus in the squirrel monkey. No response to otolith stimulation was found in this PIVC area, and the neighboring area designated as purely auditory was not investigated for electrophysiological responses during vestibular stimulation (Guldin, Akbarian, & Grusser, 1992). It is also important to acknowledge that data from non-human primates during natural vestibular stimulation on motion platforms might differ from human data during artificial vestibular stimulation (Gale et al., 2015).

We found activations in the border zone that is generally perceived as the primary auditory cortex but noise should be considered as a confounding factor. The primary auditory cortex in Heschl's gyrus is particularly well studied, and a tonotopic map has been defined spanning from low-frequency sound in the lateral part to high-frequency sound in the medial part of the gyrus (Saenz & Langers, 2014). However, there is a lack of agreement on the regional borders of the human primary auditory cortex in Heschl's gyrus (Morosan et al., 2001; Saenz & Langers, 2014). Our study participants wore noise-canceling headsets to reduce auditory stimulation. Also, we measured no discernible high-frequency sound and only low levels of low-frequency sound when the chair moved (Supporting Information Figure S2). Nevertheless, the optimal way to exclude the possibility that our finding was fully or partly caused by auditory stimulation would be to perform an additional ^{18}F -FDG PET scan in all subjects during pure auditory stimulation and compare those results with the vestibular stimulation scans. Regrettably, we were not permitted to perform such scans due to radiation concerns, as we were only allowed to perform three scans per subject. However, we did compare the present results with those from clinical language stimulation studies. At our PET department, such language stimulation studies are frequently performed using a ^{15}O - H_2O perfusion PET scans. Human speech is low frequency (250–4000 Hz) and gives rise to very robust activation of the primary auditory cortex. However, such activity is always located in the lateral aspects of Heschl's gyrus remote from the activation foci produced by the present vestibular paradigm (Supporting Information Figure S3). Although this language activation data set is based on perfusion PET rather than glucose uptake, it has been consistently shown that activation-induced increases in

perfusion and ^{18}F -FDG uptake are tightly linked (Hoge & Pike, 2001; Raichle, Grubb, Gado, Eichling, & Ter-Pogossian, 1976; Sokoloff, 1981) and spatially colocalized increases in perfusion and glucose uptake have been reported following, for example, visual and somatosensory cortex stimulation paradigms (Fox, Raichle, Mintun, & Dence, 1988; Ginsberg et al., 1988). For these reasons, we find it unlikely that the activity found in Heschl's gyrus was caused by auditory stimulation. Friberg et al. also found a close relationship between the auditory and vestibular cortical areas after attempting to control for auditory stimulus during caloric vestibular stimulation (Friberg, Olsen, Roland, Paulson, & Lassen, 1985). Notably, loud sound is also a vestibular stimulus, and thus, neuroimaging studies that use relatively loud sounds to study auditory cortices could theoretically be biased by confounding vestibular activation (Curthoys, 2017).

It has been established for decades that increases in perfusion and ^{18}F -FDG uptake are generally tightly coupled and show anatomical colocalization across various stimulation paradigms (Hoge & Pike, 2001; Raichle et al., 1976; Sokoloff, 1977, 1981). We naturally cannot rule out that this is not in vestibular stimulation, although such colocalization has been observed in stimulation paradigms of other primary senses, including vision and somatosensory stimulation (Fox et al., 1988; Ginsberg et al., 1988).

The labyrinth in the inner ear is complex of fluid-filled canals and cavities that arise from a single shared region of the otocyst during embryogenesis (Morsli, Choo, Ryan, Johnson, & Wu, 1998). The labyrinth contains both the vestibular organ and cochlea and they share structural and functional similarities, including the principle of viscous fluids stimulating mechanoreceptor hair cells to detect motion, orientation, and sound. Information from the mechanoreceptor hair cells in both the vestibular part and cochlea are transported to central nervous system via the eighth cranial nerve. Therefore, it is likely that the primary vestibular cortex could be closely integrated with the auditory cortex in Heschl's gyrus in humans. Of particular interest, a cytoarchitectonic study has demonstrated clear subdivisions within Heschl's gyrus, suggesting that it could be processing more than one type of input (Morosan et al., 2001).

In addition to Heschl's gyrus, the clusters of significantly activated voxels also overlapped with the posterior insula, thus supporting the hypothesis that this structure is a core region in vestibular processing (Lopez & Blanke, 2011; zu Eulenburg et al., 2012). The posterior insula appears to be multimodal and is implicated in processing a variety of stimuli (Kurth et al., 2010). It does not merely receive information from the vestibular organ but also integrates stimuli from the visual and proprioceptive systems (Shinder & Newlands, 2014). This organization may reflect the fact that vestibular information is deeply integrated with visual, auditory, and somatosensory information to produce the overall sense of orientation in space. Thus, we argue that the true *primary* vestibular cortex may be located in the medial Heschl's gyrus and that the neighboring posterior insula may represent a secondary association area, in which several sensory modalities are integrated.

Several sensory systems demonstrate specific topographic cortical representations of the peripheral sensory organs. Well-known examples of these topographic maps are the visual cortex and the somatosensory

homunculi. No prior studies have been able to make a clear cortical differentiation between otolith and semicircular canal function in humans (Dieterich & Brandt, 2018). The two types of stimuli used in the present study were chosen in order to primarily stimulate the horizontal semicircular canal (rotation of the chair) and the utricle (linear sideways movement). Dieterich et al. (2003) reported a dominance of vestibular cortical function in the nondominant hemisphere. This ^{15}O -H $_2\text{O}$ PET study during right-sided caloric stimulation demonstrated maximum activation in the ipsilateral hemisphere in right-handed participants. We were not allowed to perform more than three ^{18}F -FDG PET scans in our study subjects due to the cumulative radioactive dose imposed by these scans. For these reasons, we only included right-handed participants and explored predominantly right-sided stimuli in an attempt to create maximum cortical activation. We elected to study unidirectional rotation, clockwise (predominantly right-sided semicircular canal) and linear acceleration (predominantly right-sided utricle stimulus). Both types of stimuli are presented in comparison to a baseline scan. We found relatively uniform bilateral increases of ^{18}F -FDG in the Heschl's gyrus-posterior insula intersection during both stimulation paradigms. The cluster-derived VOI is asymmetrical located in the two hemispheres and as a consequence no statistical analysis is performed to compare the ^{18}F -FDG uptake between the cluster-derived VOI in the two hemispheres. The SPM analysis revealed clusters with increased ^{18}F -FDG uptake during the linear stimulation compared with the rotatory stimulation approach (Figure 4). The linear stimulus was probably more forceful than the rotatory stimulus, leading to some additional cortical activation, but the difference could also reflect distinct networks of cortex that were more involved during processing of linear acceleration. The increased activation in Heschl's gyrus during linear stimulation was only observed in the right hemisphere, which might be due to our asymmetrical stimulation in order to deliver a stronger stimulation to the vestibular organ on the right side (Figure 1). However, it was not possible to design a natural vestibular stimulus that solely stimulates one specific part or side of the vestibular organ. So, although efforts were made to confine each stimulation scenario to one part of the vestibular organ, other parts may have been stimulated sufficiently during the 35 min of movement to make discrimination of individual cortical areas difficult.

Careful considerations were taken to design the movement pattern, speed, and acceleration of the chair (Figure 1). An immediate challenge was to apply sufficient stimulus without provoking motion sickness during the 35 min of continuous stimulation. All trial participants were asked to report how they felt after stimulation in the chair, and none reported any kind of motion sickness or related symptoms.

Acknowledging that coactivation of other sensory systems than the vestibular organ would complicate the interpretation of the results, and efforts were made to avoid or reduce such stimulations as much as possible. The ability to maintain balance in humans relies not only on the vestibular input but also on continuous proprioceptive input and visual information. The participants wore sleep-goggles, and we did not see any activation in visual cortices. To reduce confounding motor signals from compensating skeletal muscle activation, the participants were tightly fixated to the chair including a headband. Nevertheless, significant activation was observed in the approximate

“trunk region” of the sensory-motor cortex (Figure 3), suggesting that some involuntary stabilizing muscle activity may have occurred during acceleration and deceleration, in addition to potential sensory stimulation of the trunk due to the continuously changing movements of the chair. However, alternative explanations may also be possible. Vestibular information provides basic clues to orientation in space and is important for coordinated body movements, directing attention and also stabilization of the body to counteract external forces. These functions also depend on somatosensory, auditory, and visual information as well as spatial memory. It is therefore possible that processing of vestibular information is not clearly separated from the complimentary influx of other types of sensory information.

The use of separate stimulation paradigms to study otolith and semicircular canal function in isolation would be desirable but extremely difficult in practice. Thus, we cannot rule out that our findings in the two paradigms represent somewhat overlapping stimulation of both vestibular organs.

This study visualized the vestibular cortical processing associated with natural vestibular stimulus in humans. Our results suggest that the medial part of Heschl's gyrus and the posterior insula constitute core structures for processing information from the vestibular organs. Surprisingly, the stimulus-induced ^{18}F -FDG uptake was highest in the medial Heschl's gyrus, which is assumed to subserve only processing of auditory input. Considering the neighboring localization, structural and functional similarity, and shared embryological development of the vestibular organ and cochlea, it is possible that the primary vestibular cortex could also be closely connected to and perhaps integrated into the primary auditory cortex of Heschl's gyrus. Further studies are needed to corroborate this hypothesis.

ACKNOWLEDGMENTS

Thank you to Jens Agergaard from *Jyden*, Denmark, for assistance in the development of the self-propelled chair. Steffen Ringgaard, MR Research Center, Aarhus University Hospital, is acknowledged for help during MRI acquisitions.

CONFLICT OF INTEREST

The authors declare no potential conflict of interest.

AUTHOR CONTRIBUTIONS

T.O., J.-J.M.-H., L.D., M.M., P.B., and M.P. initiated and designed the study. L.D. included and vestibular tested all trial participants. L.D. collected PET data. M.P. was responsible for collection of MRI data. C.B.C. collected auditory measurements and prepared Supporting Information Figure S2. A.K.H., P.B., L.D., and K.V.H. conducted data analysis including Tables 1 and 2. L.D., A.K.H., and P.B. wrote the main manuscript text. A.K.H., P.B., and K.V.H. prepared Figures 2–4 and Supporting Information Figure S1. L.D. prepared Figure 1. All authors reviewed the manuscript.

DATA AVAILABILITY STATEMENT

The data that support the findings of this study are available from the corresponding author upon reasonable request.

ORCID

Louise Devantier  <https://orcid.org/0000-0001-7811-4874>

REFERENCES

- Boegle, R., Stephan, T., Ertl, M., Glasauer, S., & Dieterich, M. (2016). Magnetic vestibular stimulation modulates default mode network fluctuations. *NeuroImage*, 127, 409–421. <https://doi.org/10.1016/j.neuroimage.2015.11.065>
- Chen, A., DeAngelis, G. C., & Angelaki, D. E. (2010). Macaque parieto-insular vestibular cortex: Responses to self-motion and optic flow. *The Journal of Neuroscience*, 30(8), 3022–3042. <https://doi.org/10.1523/jneurosci.4029-09.2010>
- Curthoys, I. S. (2017). The new vestibular stimuli: Sound and vibration-anatomical, physiological and clinical evidence. *Experimental Brain Research*, 235(4), 957–972. <https://doi.org/10.1007/s00221-017-4874-y>
- Curthoys, I. S., & Vulovic, V. (2011). Vestibular primary afferent responses to sound and vibration in the Guinea pig. *Experimental Brain Research*, 210(3–4), 347–352. <https://doi.org/10.1007/s00221-010-2499-5>
- Desikan, R. S., Segonne, F., Fischl, B., Quinn, B. T., Dickerson, B. C., Blacker, D., ... Killiany, R. J. (2006). An automated labeling system for subdividing the human cerebral cortex on MRI scans into gyral based regions of interest. *NeuroImage*, 31(3), 968–980. <https://doi.org/10.1016/j.neuroimage.2006.01.021>
- Dieterich, M., Bense, S., Lutz, S., Drzezga, A., Stephan, T., Bartenstein, P., & Brandt, T. (2003). Dominance for vestibular cortical function in the non-dominant hemisphere. *Cerebral Cortex*, 13(9), 994–1007. <https://doi.org/10.1093/cercor/13.9.994>
- Dieterich, M., & Brandt, T. (2018). The parietal lobe and the vestibular system. *Handbook of Clinical Neurology*, 151, 119–140. <https://doi.org/10.1016/b978-0-444-63622-5.00006-1>
- Fox, P. T., Raichle, M. E., Mintun, M. A., & Dence, C. (1988). Nonoxidative glucose consumption during focal physiologic neural activity. *Science*, 241(4864), 462–464. <https://doi.org/10.1126/science.3260686>
- Friberg, L., Olsen, T. S., Roland, P. E., Paulson, O. B., & Lassen, N. A. (1985). Focal increase of blood flow in the cerebral cortex of man during vestibular stimulation. *Brain*, 108(Pt 3), 609–623. <https://doi.org/10.1093/brain/108.3.609>
- Gale, S., Prsa, M., Schurger, A., Gay, A., Paillard, A., Herbelin, B., ... Blanke, O. (2015). Oscillatory neural responses evoked by natural vestibular stimuli in humans. *J Neurophysiol*, 115, 1228–1242. <https://doi.org/10.1152/jn.00153.2015>
- Ginsberg, M. D., Chang, J. Y., Kelley, R. E., Yoshii, F., Barker, W. W., Ingenito, G., & Boothe, T. E. (1988). Increases in both cerebral glucose utilization and blood flow during execution of a somatosensory task. *Annals of Neurology*, 23(2), 152–160. <https://doi.org/10.1002/ana.410230208>
- Grusser, O. J., Pause, M., & Schreiter, U. (1990a). Localization and responses of neurones in the parieto-insular vestibular cortex of awake monkeys (*Macaca fascicularis*). *The Journal of Physiology*, 430, 537–557. <https://doi.org/10.1113/jphysiol.1990.sp018306>
- Grusser, O. J., Pause, M., & Schreiter, U. (1990b). Vestibular neurones in the parieto-insular cortex of monkeys (*Macaca fascicularis*): Visual and neck receptor responses. *The Journal of Physiology*, 430, 559–583. <https://doi.org/10.1113/jphysiol.1990.sp018307>

- Guldin, W. O., Akbarian, S., & Grusser, O. J. (1992). Cortico-cortical connections and cytoarchitectonics of the primate vestibular cortex: A study in squirrel monkeys (*Saimiri sciureus*). *The Journal of Comparative Neurology*, 326(3), 375–401. <https://doi.org/10.1002/cne.903260306>
- Guldin, W. O., & Grusser, O. J. (1998). Is there a vestibular cortex? *Trends in Neurosciences*, 21(6), 254–259. [https://doi.org/10.1016/S0166-2236\(97\)01211-3](https://doi.org/10.1016/S0166-2236(97)01211-3)
- Hagler, D. J., Jr., Saygin, A. P., & Sereno, M. I. (2006). Smoothing and cluster thresholding for cortical surface-based group analysis of fMRI data. *NeuroImage*, 33(4), 1093–1103. <https://doi.org/10.1016/j.neuroimage.2006.07.036>
- Halmagyi, G. M., Chen, L., MacDougall, H. G., Weber, K. P., McGarvie, L. A., & Curthoys, I. S. (2017). The video head impulse test. *Frontiers in Neurology*, 8, 258. <https://doi.org/10.3389/fneur.2017.00258>
- Heiss, W. D., Habedank, B., Klein, J. C., Herholz, K., Wienhard, K., Lenox, M., & Nutt, R. (2004). Metabolic rates in small brain nuclei determined by high-resolution PET. *Journal of Nuclear Medicine*, 45(11), 1811–1815.
- Hoge, R. D., & Pike, G. B. (2001). Oxidative metabolism and the detection of neuronal activation via imaging. *Journal of Chemical Neuroanatomy*, 22(1–2), 43–52. [https://doi.org/10.1016/S0891-0618\(01\)00114-4](https://doi.org/10.1016/S0891-0618(01)00114-4)
- Jeong, M., Tashiro, M., Singh, L. N., Yamaguchi, K., Horikawa, E., Miyake, M., ... Itoh, M. (2006). Functional brain mapping of actual car-driving using [18F]FDG-PET. *Annals of Nuclear Medicine*, 20(9), 623–628. <https://doi.org/10.1007/BF02984660>
- Kameyama, M., Murakami, K., & Jinzaki, M. (2016). Comparison of [(15)O] H₂O positron emission tomography and functional magnetic resonance imaging in activation studies. *World Journal of Nuclear Medicine*, 15(1), 3–6. <https://doi.org/10.4103/1450-1147.172139>
- Kurth, F., Eickhoff, S. B., Schleicher, A., Hoemke, L., Zilles, K., & Amunts, K. (2010). Cytoarchitecture and probabilistic maps of the human posterior insular cortex. *Cerebral Cortex*, 20(6), 1448–1461. <https://doi.org/10.1093/cercor/bhp208>
- Lopez, C., & Blanke, O. (2011). The thalamocortical vestibular system in animals and humans. *Brain Research Reviews*, 67(1–2), 119–146. <https://doi.org/10.1016/j.brainresrev.2010.12.002>
- Mian, O. S., Li, Y., Antunes, A., Glover, P. M., & Day, B. L. (2013). On the vertigo due to static magnetic fields. *PLoS One*, 8(10), e78748. <https://doi.org/10.1371/journal.pone.0078748>
- Morosan, P., Rademacher, J., Schleicher, A., Amunts, K., Schormann, T., & Zilles, K. (2001). Human primary auditory cortex: Cytoarchitectonic subdivisions and mapping into a spatial reference system. *NeuroImage*, 13(4), 684–701. <https://doi.org/10.1006/nimg.2000.0715>
- Morsli, H., Choo, D., Ryan, A., Johnson, R., & Wu, D. K. (1998). Development of the mouse inner ear and origin of its sensory organs. *The Journal of Neuroscience*, 18(9), 3327–3335. <https://doi.org/10.1523/JNEUROSCI.18-09-03327>
- Oldfield, R. C. (1971). The assessment and analysis of handedness: The Edinburgh inventory. *Neuropsychologia*, 9(1), 97–113. [https://doi.org/10.1016/0028-3932\(71\)90067-4](https://doi.org/10.1016/0028-3932(71)90067-4)
- Raichle, M. E., Grubb, R. L., Jr., Gado, M. H., Eichling, J. O., & Ter-Pogossian, M. M. (1976). Correlation between regional cerebral blood flow and oxidative metabolism. in vivo studies in man. *Archives of Neurology*, 33(8), 523–526. <https://doi.org/10.1121/1.1310190>
- Ravicz, M. E., & Melcher, J. R. (2001). Isolating the auditory system from acoustic noise during functional magnetic resonance imaging: Examination of noise conduction through the ear canal, head, and body. *The Journal of the Acoustical Society of America*, 109(1), 216–231. <https://doi.org/10.1121/1.1326083>
- Roberts, D. C., Marcelli, V., Gillen, J. S., Carey, J. P., Della Santina, C. C., & Zee, D. S. (2011). MRI magnetic field stimulates rotational sensors of the brain. *Current Biology*, 21(19), 1635–1640. <https://doi.org/10.1016/j.cub.2011.08.029>
- Saenz, M., & Langers, D. R. (2014). Tonotopic mapping of human auditory cortex. *Hearing Research*, 307, 42–52. <https://doi.org/10.1016/j.heares.2013.07.016>
- Shinder, M. E., & Newlands, S. D. (2014). Sensory convergence in the parieto-insular vestibular cortex. *Journal of Neurophysiology*, 111(12), 2445–2464. <https://doi.org/10.1152/jn.00731.2013>
- Sokoloff, L. (1977). Relation between physiological function and energy metabolism in the central nervous system. *Journal of Neurochemistry*, 29(1), 13–26. <https://doi.org/10.1111/j.1471-4159.1977.tb03919.x>
- Sokoloff, L. (1981). Relationships among local functional activity, energy metabolism, and blood flow in the central nervous system. *Federation Proceedings*, 40(8), 2311–2316.
- Tashiro, M., Itoh, M., Fujimoto, T., Fujiwara, T., Ota, H., Kubota, K., ... Sasaki, H. (2001). 18F-FDG PET mapping of regional brain activity in runners. *The Journal of Sports Medicine and Physical Fitness*, 41(1), 11–17.
- Varrone, A., Asenbaum, S., Vander Borgh, T., Booi, J., Nobili, F., Nagren, K., ... Van Laere, K. (2009). EANM procedure guidelines for PET brain imaging using [18F]FDG, version 2. *European Journal of Nuclear Medicine and Molecular Imaging*, 36(12), 2103–2110. <https://doi.org/10.1007/s00259-009-1264-0>
- Villien, M., Wey, H. Y., Mandeville, J. B., Catana, C., Polimeni, J. R., Sander, C. Y., ... Hooker, J. M. (2014). Dynamic functional imaging of brain glucose utilization using fPET-FDG. *NeuroImage*, 100, 192–199. <https://doi.org/10.1016/j.neuroimage.2014.06.025>
- von Elm, E., Altman, D. G., Egger, M., Pocock, S. J., Gøtzsche, P. C., & Vandenbroucke, J. P. (2014). The strengthening the reporting of observational studies in epidemiology (STROBE) statement: Guidelines for reporting observational studies. *International Journal of Surgery*, 12(12), 1495–1499. <https://doi.org/10.1016/j.ijssu.2014.07.013>
- Ward, B. K., Roberts, D. C., Della Santina, C. C., Carey, J. P., & Zee, D. S. (2015). Vestibular stimulation by magnetic fields. *Annals of the New York Academy of Sciences*, 1343, 69–79. <https://doi.org/10.1111/nyas.12702>
- zu Eulenburg, P., Caspers, S., Roski, C., & Eickhoff, S. B. (2012). Meta-analytical definition and functional connectivity of the human vestibular cortex. *NeuroImage*, 60(1), 162–169. <https://doi.org/10.1016/j.neuroimage.2011.12.032>
- zu Eulenburg, P., Müller-Forell, W., & Dieterich, M. (2013). On the recall of vestibular sensations. *Brain Structure & Function*, 218(1), 255–267. <https://doi.org/10.1007/s00429-012-0399-0>

SUPPORTING INFORMATION

Additional supporting information may be found online in the Supporting Information section at the end of this article.

How to cite this article: Devantier L, Hansen AK, Mølby-Henriksen J-J, et al. Positron emission tomography visualized stimulation of the vestibular organ is localized in Heschl's gyrus. *Hum Brain Mapp*. 2020;41:185–193. <https://doi.org/10.1002/hbm.24798>